Form factors of pion and kaon

Jun Gao and Bing An Li

Department of Physics and Astronomy, University of Kentucky

Lexington, KY 40506, USA

Abstract

Besides the vector meson poles in the form factors of charged pion and kaons additional intrinsic form factors of pion and kaons are found. A detailed study of the form factors of pion and kaons in both time-like and space-like regions is presented. Theory agrees well with data up to $q \sim 1.4GeV$. In this study there is no adjustable parameter.

Form factor is a very important physical quantity in understanding the internal structure of hadrons. The vector meson dominance (VMD)[1] is successful in studying electromagnetic interactions and the vector part of weak interactions of mesons. According to the VMD the pion form factor is determined by a $\rho-$meson pole[2]. Generally speaking, the $\rho-$ pole fits the data pretty well. However, a detailed study shows that there is deviation between the experimental data of the pion form factor and the $\rho-$pole. The electromagnetic radius of charged pion has been determined to be[3]

$$< r^2 >_\pi^{exp}= (0.439 \pm 0.03) fm^2, \tag{1}$$

whereas the result obtained from ρ-pole is

$$< r^2 >_\pi^{\rho-pole}= 0.391 fm^2. \tag{2}$$

In Ref.[4] a comparison between the measurements and the $\rho-$ pole[2] of the pion form factor is presented. The Fig.6.3 of Ref.[4] shows that the $\rho-$ pole[2] decreases a little bit faster in time-like region and slower in space-like region. The experiments show that besides the $\rho-$ pole maybe an additional form factor is needed.

Based on t'Hooft's arguments that in large N_C limit QCD is equivalent to a meson theory[5] an effective chiral theory of large N_C QCD of mesons has been proposed[6]. It has been shown that the tree diagrams of mesons are at leading orders and the loop diagrams of mesons are at higher orders in large N_C expansion. In chiral limit, $m_q \to 0$, the Lagrangian of this theory in the case of two flavors takes the form

$$\begin{aligned}\mathcal{L} &= \overline{\psi}(x)[i\gamma\cdot\partial+\gamma\cdot v+\gamma\cdot a\gamma_5-mu(x)]\psi(x)\\ &+\frac{1}{2}m_0^2(\rho_i^\mu\rho_{\mu i}+\omega^\mu\omega_\mu+a_i^\mu a_{\mu i}+f^\mu f_\mu),\end{aligned}\tag{3}$$

where $a_\mu=\tau_i a_\mu^i+f_\mu, v_\mu=\tau_i\rho_\mu^i+\omega_\mu$, and $u=exp\{i\gamma_5(\tau_i\pi_i+\eta)\}$; m is a parameter; u can be written as

$$u=\frac{1}{2}(1+\gamma_5)U+\frac{1}{2}(1-\gamma_5)U^+,\quad U=exp\{i(\tau_i\pi_i+\eta)\}.$$

The photon A, W and Z fields can be incorporated to the Lagrangian as well. In terms of path integral the effective Lagrangian of mesons is obtained by integrating out the quark fields. All the details can be found in Ref.[6]. The effective Lagrangian has been applied to study meson physics[7,8]. Theoretical results agree well with data.

The VMD is a natural result of this theory[6] and the expressions of the VMD (ρ, ω, and ϕ) are derived

$$\begin{aligned}&\frac{1}{2}eg\{-\frac{1}{2}F^{\mu\nu}(\partial_\mu\rho_\nu^0-\partial_\nu\rho_\mu^0)+A^\mu j_\mu^0\},\\ &\frac{1}{6}eg\{-\frac{1}{2}F^{\mu\nu}(\partial_\mu\omega_\nu-\partial_\nu\omega_\mu)+A^\mu j_\mu^\omega\},\\ &-\frac{1}{3\sqrt{2}}eg\{-\frac{1}{2}F^{\mu\nu}(\partial_\mu\phi_\nu-\partial_\nu\phi_\mu)+A^\mu j_\mu^\phi\},\end{aligned}\tag{4}$$

g is a universal coupling constant in this theory and has been determined to be 0.39 by fitting $\rho\to ee^+$ ($\Gamma^{th}=6.53keV$ and $\Gamma^{ex}=(6.77\pm0.32)keV$). The current j_μ^0 is derived from the vertex of $\rho\pi\pi$[6]

$$\mathcal{L}_{\rho\pi\pi} = \frac{2}{g} f_{\rho\pi\pi}(q^2)\epsilon_{ijk}\rho_i^\mu \pi_j \partial_\mu \pi_k \tag{5}$$

by substituting

$$\rho_\mu^0 \rightarrow \frac{1}{2} e g A_\mu$$

into Eq.(5), where

$$f_{\rho\pi\pi}(q^2) = 1 + \frac{q^2}{2\pi^2 f_\pi^2}[(1 - \frac{2c}{g})^2 - 4\pi^2 c^2] = 1 + 0.243(q^2/GeV^2) \tag{6}$$

where $c = \frac{f_\pi^2}{2gm_\rho^2}$, $f_\pi = 0.186GeV$, $m_\rho = 0.773GeV$ and q is the momentum of ρ meson. $f_{\rho\pi\pi}(q^2)$ is determined up to the fourth order in derivatives. It is necessary to emphasize that the VMD(4) is derived from this theory, however, the $\rho\pi\pi$ coupling in this theory is no longer a constant. There is a function $f_{\rho\pi\pi}(q^2)$ in the vertex $\mathcal{L}_{\rho\pi\pi}$. $f_{\rho\pi\pi}(q^2)$ is the intrinsic form factor of pion. The intrinsic form factor is the physical effect of quark loops. There are intrinsic form factors for kaons too(see below). In this paper we apply VMD(4) in which an intrinsic form factor is included to study form factors of pion and kaons. A detailed comparison between theoretical results of the form factors and experimental data in both time-like and space-like regions is presented.

The VMD(4) shows that the pion form factor is determined by two Feynman diagrams shown in Fig.1 and obtained from Eqs.(4,5,6)

$$|F_\pi(q^2)|^2 = f_{\rho\pi\pi}^2(q^2)\frac{m_\rho^4 + q^2\Gamma_\rho^2(q^2)}{(q^2 - m_\rho^2)^2 + q^2\Gamma_\rho^2(q^2)} \tag{7}$$

in time-like region, where $\Gamma_\rho(q^2)$ is the decay width of ρ meson.

$$
\begin{aligned}
\Gamma_\rho(q^2) &= \Gamma_{\rho^0\to\pi^+\pi^-}(q^2)+\Gamma_{\rho^0\to K\overline{K}}(q^2),\\
\Gamma_{\rho^0\to\pi^+\pi^-}(q^2) &= \frac{f^2_{\rho\pi\pi}(q^2)\sqrt{q^2}}{12\pi g^2}(1-\frac{4m^2_{\pi^+}}{q^2})^{\frac{3}{2}}\theta(q^2>4m^2_{\pi^+}),\\
\Gamma_{\rho^0\to K\bar{K}}(q^2) &= \frac{f^2_{\rho\pi\pi}(q^2)\sqrt{q^2}}{48\pi g^2}(1-\frac{4m^2_{K^+}}{q^2})^{\frac{3}{2}}\theta(q^2>4m^2_{K^+})\\
&\quad+\frac{f^2_{\rho\pi\pi}(q^2)\sqrt{q^2}}{48\pi g^2}(1-\frac{4m^2_{K^0}}{q^2})^{\frac{3}{2}}\theta(q^2>4m^2_{K^0}),
\end{aligned}
\tag{8}
$$

when $q^2 > 4m^2_{K^+}$ the $K\bar{K}$ channel is open. There are other channels, however, in the range of $\sqrt{q^2} < 1.4GeV$ the contribution of other channels is negligible. In space-like region the pion form factor is

$$
F_\pi(q^2)=\frac{m^2_\rho f_{\rho\pi\pi}(q^2)}{m^2_\rho-q^2}. \tag{9}
$$

From Eqs.(7,9) it can be seen that the pion form factor consists of two parts: the intrinsic form factor $f_{\rho\pi\pi}(q^2)$(6) and the $\rho-$ pole. The expression of $f_{\rho\pi\pi}(q^2)$ shows that in time-like region $f_{\rho\pi\pi}(q^2)$ increases with q^2 and in space-like region it decreases with q^2. As mention above this behavior is needed to fit the data.

In time-like region the pion form factor has been measured in $ee^+\to\pi\pi$ and $\tau\to\pi\pi\nu$. The cross section of $ee^+\to\pi^+\pi^-$ is expressed as

$$
\sigma = \frac{\pi\alpha^2}{3}\frac{1}{q^2}(1-\frac{4m^2_{\pi^+}}{q^2})^{\frac{3}{2}}|F_\pi(q^2)|^2. \tag{10}
$$

Taking $\rho - \omega$ mixing into account we obtain

$$F_\pi(q^2) = f_{\rho\pi\pi}(q^2)\{1 - \frac{q^2 \cos\theta}{q^2 - m_\rho^2 + i\sqrt{q^2}\Gamma_\rho(q^2)} - \frac{1}{3}\frac{q^2 \sin\theta}{q^2 - m_\omega^2 + i\sqrt{q^2}\Gamma_\omega}\}, \tag{11}$$

where θ is the mixing angle and determined to be 1.74^0 in Ref.[6]. From Eq.(11), the pion form factor with $\rho - \omega$ mixing in space-like region is obtained

$$F_\pi(q^2) = f_{\rho\pi\pi}(q^2)\{1 - \frac{q^2 \cos\theta}{q^2 - m_\rho^2} - \frac{1}{3}\frac{q^2 \sin\theta}{q^2 - m_\omega^2}\}. \tag{12}$$

The comparison of the cross section(10), the form factor of pion in both time-like and space-like regions(11-12) with data are shown in Fig.2-5. Up to $\sqrt{q^2} = 1.4GeV$ the channel $\rho \to \pi\pi$ is dominant and the contribution of the $K\bar{K}$ mode is very small. The intrinsic form factor $f_{\rho\pi\pi}(q^2)$ plays more important role in the range of higher q^2. Using Eq.(8), we obtain $\Gamma_\rho = 143.2MeV$ which fits the data well(see Fig.2,3). $f^2_{\rho\pi\pi}(q^2) = 1.31$ at $q^2 = m^2_\rho$, therefore, the intrinsic form factor makes significant contribution to Γ_ρ. In Ref.[9] a fitting of ρ resonance to $ee^+ \to \pi\pi$ has been presented. The radius of charged pion is found from Eq.(12)

$$< r^2 >_\pi = 6(\frac{\cos\theta}{m_\rho^2} + \frac{\sin\theta}{3m_\omega^2}) + \frac{3}{\pi^2 f_\pi^2}\{(1 - \frac{2c}{g})^2 - 4\pi^2 c^2\}. \tag{13}$$

The numerical result is

$$< r^2 >_\pi = (0.395 + 0.057) fm^2 = 0.452 fm^2, \tag{14}$$

where the first number 0.395 comes from ρ and ω poles and the second is the contribution of the intrinsic form factor(6), which is about 13% of the total value. The experimental data is $(0.439 \pm 0.03) fm^2$ [3].

In terms of the method presented in Ref.[7], the decay rate of $\tau \to \pi\pi\nu$ is derived

$$\frac{d\Gamma}{dq^2} = \frac{G^2}{(2\pi)^3}\frac{\cos^2\theta_C}{48m_\tau^3}(m_\tau^2 + 2q^2)(m_\tau^2 - q^2)^2\{1 - \frac{4m_\pi^2}{q^2}\}^{3/2}|F_\pi(q^2)|^2, \tag{15}$$

where $F_\pi(q^2)$ is given by Eq.(7). In Ref.[10] it is shown that the form factor $F_\pi(q^2)$ determined from τ decay is consistent with the one obtained from ee^+ annihilation. The branching ratio is calculated to be

$$B_{\tau^- \to \pi^0\pi^-\nu_\tau} = 22.3\%. \tag{16}$$

The experimental data is $B_{\tau^- \to \pi^0\pi^-\nu_\tau} = (25.32 \pm 0.15)\%$[11].

In the same way the form factors of charged and neutral kaons are studied. All the three vector mesons, ρ, ω, and ϕ, contribute to the form factors of kaons. Using the substitutions

$$\phi_\mu \longrightarrow -\frac{eg}{3\sqrt{2}}A_\mu, \quad \omega_\mu \longrightarrow \frac{eg}{6}A_\mu, \tag{17}$$

the currents $j_\mu^{\omega,\phi}$ of Eq.(4) are obtained from the vertices[6]

$$\begin{aligned}\mathcal{L}_{vK\overline{K}} = & -\frac{2\sqrt{2}}{g}if_{\rho\pi\pi}(q^2)\phi^\mu(K^+\partial_\mu K^- + K^0\partial_\mu\overline{K^0}) \\ & +\frac{2}{g}if_{\rho\pi\pi}(q^2)\omega^\mu(K^+\partial_\mu K^- + K^0\partial_\mu\overline{K^0}) \\ & +\frac{2}{g}if_{\rho\pi\pi}(q^2)\rho^\mu(K^+\partial_\mu K^- - K^0\partial_\mu\overline{K^0}).\end{aligned} \tag{18}$$

The cross sections of $e^+e^- \longrightarrow K^+K^-$ and $e^+e^- \longrightarrow K^0\overline{K^0}$ are derived

$$\begin{aligned}
\sigma_{e^+e^-\to K^+K^-} &= \frac{\pi\alpha^2}{3}\frac{1}{q^2}(1-\frac{4m^2_{K^+}}{q^2})^{\frac{3}{2}}|F_{K^+}|^2, \\
\sigma_{e^+e^-\to K^0\overline{K^0}} &= \frac{\pi\alpha^2}{3}\frac{1}{q^2}(1-\frac{4m^2_{K^0}}{q^2})^{\frac{3}{2}}|F_{K^0}|^2,
\end{aligned} \tag{19}$$

where

$$|F_{K^+}(q^2)|^2 = f^2_{\rho\pi\pi}(q^2)|A|^2, \tag{20}$$

$$|F_{K^0}(q^2)|^2 = f^2_{\rho\pi\pi}(q^2)|B|^2. \tag{21}$$

A and B are defined as

$$\begin{aligned}
A &= \frac{1}{2}\frac{-m^2_\rho + i\sqrt{q^2}\Gamma_\rho(q^2)}{q^2 - m^2_\rho + i\sqrt{q^2}\Gamma_\rho(q^2)} + \frac{1}{6}\frac{-m^2_\omega + i\sqrt{q^2}\Gamma_\omega}{q^2 - m^2_\omega + i\sqrt{q^2}\Gamma_\omega}, \\
&+\frac{1}{3}\frac{-m^2_\phi + i\sqrt{q^2}\Gamma_\phi(q^2)}{q^2 - m^2_\phi + i\sqrt{q^2}\Gamma_\phi(q^2)},
\end{aligned} \tag{22}$$

$$\begin{aligned}
B &= -\frac{1}{2}\frac{-m^2_\rho + i\sqrt{q^2}\Gamma_\rho(q^2)}{q^2 - m^2_\rho + i\sqrt{q^2}\Gamma_\rho(q^2)} + \frac{1}{6}\frac{-m^2_\omega + i\sqrt{q^2}\Gamma_\omega}{q^2 - m^2_\omega + i\sqrt{q^2}\Gamma_\omega}, \\
&+\frac{1}{3}\frac{-m^2_\phi + i\sqrt{q^2}\Gamma_\phi(q^2)}{q^2 - m^2_\phi + i\sqrt{q^2}\Gamma_\phi(q^2)}
\end{aligned} \tag{23}$$

with

$$\begin{aligned}
\Gamma_\phi(q^2) &= \Gamma_{\phi\to K^+K^-}(q^2) + \Gamma_{\phi\to K^0\overline{K^0}}(q^2), \\
\Gamma_{\phi\to K^+K^-}(q^2) &= \frac{\sqrt{q^2}}{24g^2\pi}f^2_{\rho\pi\pi}(q^2)(1-\frac{4m^2_{K^+}}{q^2})^{\frac{3}{2}}, \\
\Gamma_{\phi\to K^0\overline{K^0}}(q^2) &= \frac{\sqrt{q^2}}{24g^2\pi}f^2_{\rho\pi\pi}(q^2)(1-\frac{4m^2_{K^0}}{q^2})^{\frac{3}{2}}.
\end{aligned} \tag{24}$$

The numerical results are

$$\begin{aligned}\Gamma(\phi\rightarrow K^+K^-) &= 2.14MeV, \quad \Gamma(\phi\rightarrow K^0\overline{K}^0)=1.4MeV,\\ \Gamma(\phi\rightarrow K^+K^-)_{exp} &= 2.18(1\pm 0.028)MeV,\\ \Gamma(\phi\rightarrow K^0\bar{K}^0)_{exp} &= 1.51(1\pm 0.029)MeV. \end{aligned} \tag{25}$$

$f^2_{\rho\pi\pi}(q^2)=1.57$ at $q^2=m^2_\phi$. The contribution of the intrinsic forn factor is significant. Theoretical results of Γ_ϕ agree with the data very well. Γ_ω has been calculated to be 7.7MeV[7] which is consistent with the data 7.49(1 ± 0.02)MeV.

The cross sections of $ee^+\rightarrow K\bar{K}$ and the form factors of kaons in time-like region are shown in Fig.6-9.

The form factors of kaons in space-like region are obtained from Eqs.(20-23)

$$\begin{aligned}F_{K^+}(q^2) &= f_{\rho\pi\pi}(q^2)\{\frac{1}{2}\frac{m^2_\rho}{m^2_\rho-q^2}+\frac{1}{6}\frac{m^2_\omega}{m^2_\omega-q^2}+\frac{1}{3}\frac{m^2_\phi}{m^2_\phi-q^2}\},\\ F_{K^0}(q^2) &= f_{\rho\pi\pi}(q^2)\{-\frac{1}{2}\frac{m^2_\rho}{m^2_\rho-q^2}+\frac{1}{6}\frac{m^2_\omega}{m^2_\omega-q^2}+\frac{1}{3}\frac{m^2_\phi}{m^2_\phi-q^2}\}. \end{aligned} \tag{26}$$

The form factor, $F_{K^+}(q^2)$, is shown in Fig.10. The radius of the charged kaon is derived from Eq.(26)

$$<r^2>_{K^+} = \frac{3}{\pi^2 f^2_\pi}\{(1-\frac{2c}{g})^2-4\pi^2c^2\}+(\frac{3}{m^2_\rho}+\frac{2}{m^2_\phi}+\frac{1}{m^2_\omega}). \tag{27}$$

The numerical value is

$$<r^2>_{K^+}=(0.05+0.33)fm^2=0.38fm^2. \tag{28}$$

The first number comes from the intrinsic form factor. The experimental data is $(0.34 \pm 0.05)fm^2$ [16]. The radius of the neutral kaon is obtained from Eq.(26)

$$< r^2 >_{K^0} = -6\frac{\partial F_{K^0}(q^2)}{\partial q^2} |_{q^2=0} = -\frac{2}{m_{\phi^2}} - \frac{1}{m_\omega^2} + \frac{3}{m_\rho^2} = 0.057fm^2. \tag{29}$$

Only the coupling of $\rho K\bar{K}$ in Eq.(18) contributes to $\tau^- \to K^0 K^- \nu$. The decay rate is found to be

$$\frac{d\Gamma}{dq^2} = \frac{G^2}{(2\pi)^3}\frac{\cos^2\theta_C}{96m_\tau^3}(m_\tau^2 + 2q^2)(m_\tau^2 - q^2)^2\{1 - \frac{4m_K^2}{q^2}\}^{3/2}|F_\pi(q^2)|^2, \tag{30}$$

where $F_\pi(q^2)$ is given by Eq.(7). The theory predicts that the decay rate of this process is determined by the pion form factor in the chiral limit. So far there is no measurement on this distribution. The branching ratio of this decay mode is calculated to be

$$B_{\tau^- \longrightarrow K^0 K^- \nu_\tau} = 1.78 \times 10^{-3}. \tag{31}$$

The experimental data is $(1.59 \pm 0.24) \times 10^{-3}$[11]. Theory agrees with the data within the error bar.

In summary, the VMD derived from the chiral theory[6] has been applied to study the form factors of pion and kaons. An intrinsic form factor has been predicted by this chiral theory[6]. It has been found that this intrinsic form factor makes significant contribution to the form factors of pion and kaons, the decay widths of ρ and ϕ mesons, and the decays $\tau \to \pi\pi\nu$ and $\tau \to K\bar{K}\nu$. The theory agrees well with the data. It is necessary to point out that there is no new parameter in this study. In this theory derivative expansion is used and all the calculations are done up to the fourth order in derivatives. The fitting shows that the pion form factor is in agreement with data up to $q \sim 1.4 GeV$ in time-like region(Fig.2,3). In the range of higher q^2 the contribution of higher order derivatives should be taken into account. We will provide the study in the near future.

The study is supported by DOE grant No.DE-91ER75661.

References

[1] J.J. Sakurai, *Currents and Mesons* (University of Chicago Press, Chicago, 1969).

[2] G.J. Gounaris and J.J. Sakurai, Phys. Rev. Lett. **21**, 244 (1968).

[3] E.B. Dally et al., Phys. Rev. Lett. **48**, 375 (1982).

[4] E. Amaldi, S. Fubini and G. Furlan, *Pion-Electroproduction* (Springer-Verlag, Berlin, Heidelberg, New York, 1979).

[5] G.'t Hooft, Nucl. Phys. **B75**, 461(1974).

[6] B.A. Li, Phys. Rev. D **52**, 5165(1995); **52**, 5184 (1995).

[7] B.A. Li, Phys. Rev. D **55**, 1436 (1997); **55** 1425 (1997). In the first paper the calculation of $\tau \rightarrow K\bar{K}\nu$ has an error . The correct result is provided in this paper(31).

[8] D.N. Gao, B.A. Li, and M.L. Yan, Phys. Rev. D **56**, 4115 (1997); B.A. Li, D.N. Gao, and M.L. Yan, Phys. Rev. D **58**, 094031 (1998).

[9] M.Benayoun et al., Z. Phys. C **58**, 31 (1993).

[10] J. Urheim, Nucl. Phys. **B** (proc.Suppl.) **55C** May(1997).

[11] Particle Data Group, Euro. Phys. Jour. C, Vol.3 (1998).

[12] A. Quenzer et al., Phys. Lett. **76B**, 512 (1978); L.M. Barkov et al., Nucl. Phys. **256B**, 365 (1985).

[13] C.J. Bebek et al., Phys. Rev. D **13**, 25 (1976).

[14] B.Delcourt et al., Phys. Lett. **99B**, 257 (1981); DM2 Collaboration, Z. Phys. C, **39**, 13 (1988).

[15] N.N. Achasov and A. A. Kozhevnikov, Phys. Rev. D **57**, 4334 (1998); F. Mane et al., Phys. Lett. **99B**, 261 (1981).

[16] S.R. Amendolia et al., Phys. Lett. B **178**, 435 (1986).

Figure Captions

FIG. 1. Feynman Diagrams of pion form factor.

FIG. 2. Cross Section of $e^+e^- -> \pi^+\pi^-$ vs invariant mass of $\pi\pi$. Data are from Ref.[12].

FIG. 3. Pion form factor in time-like region. Data are from [12].

FIG. 4. Pion form factor in space-like region. Data are from [13].

FIG. 5. Pion form factor in space-like region.

FIG. 6. Cross Section of $e^+e^- -> K^+K^-$ vs invariant mass of KK. Data are from [14,15].

FIG. 7. Cross Section of $e^+e^- -> K^0\overline{K^0}$ vs invariant mass of KK. Data are from [14,15].

FIG. 8. Charged kaon form factor in time-like region. Data are from [14-16].

FIG. 9. Neutral kaon form factor in time-like region. Data are from [14-16].

FIG. 10. Charged kaon form factor in space-like region.

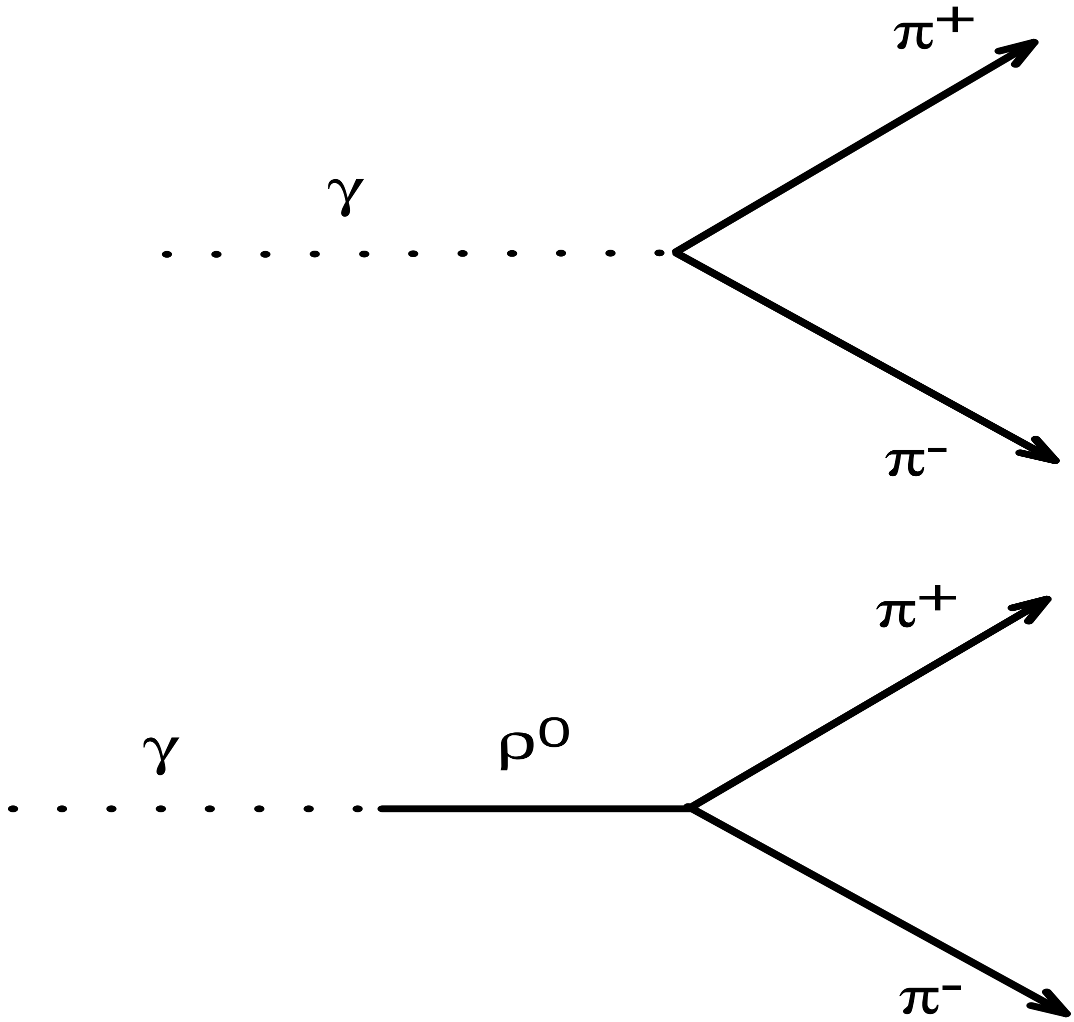

FIG. 1.

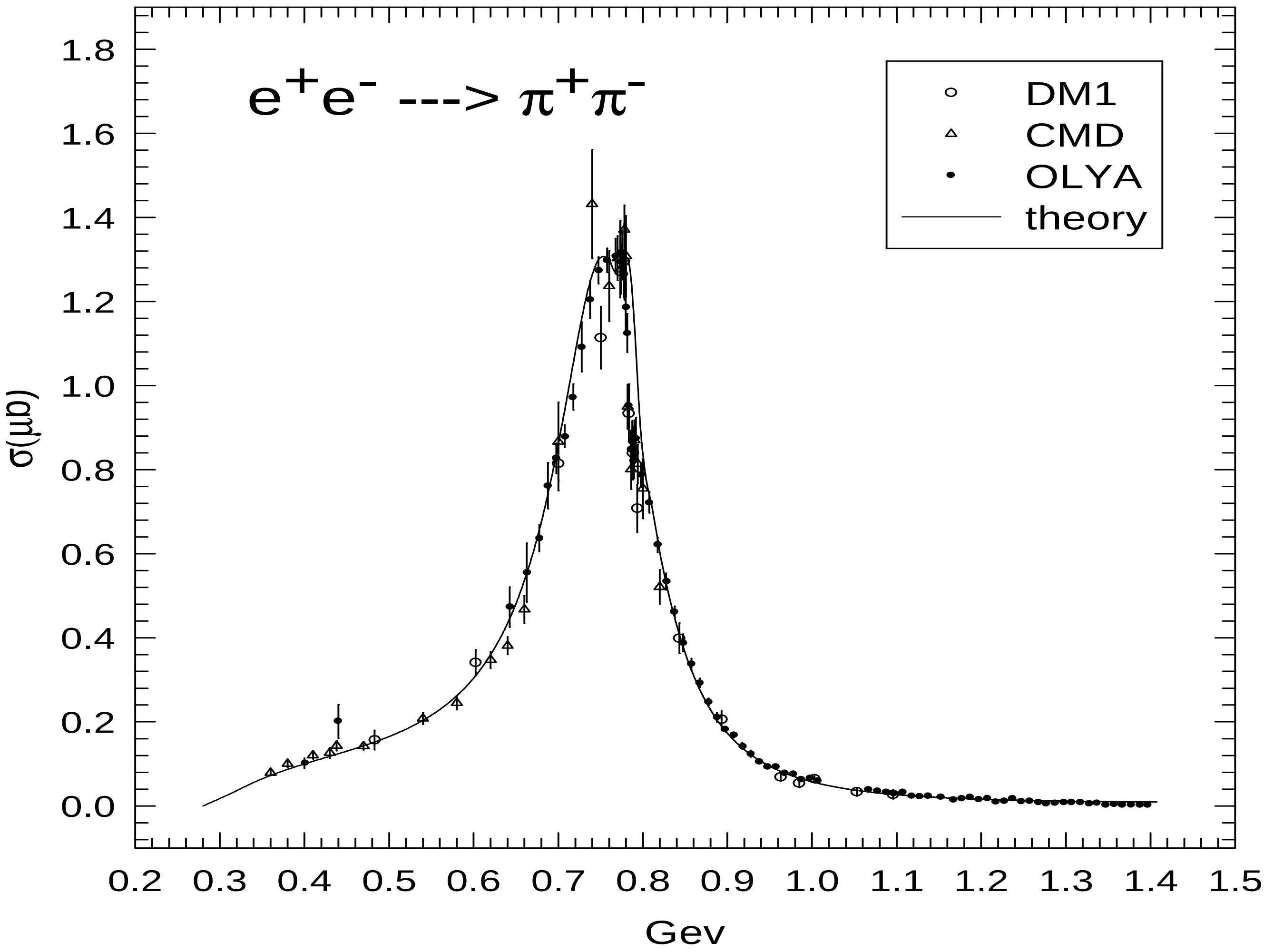

e^+e^- ---> $\pi^+\pi^-$
DM1
CMD
OLYA
theory
1.8
1.6
1.4
1.2
1.0
0.8
0.6
0.4
0.2
0.0
σ(μb)
0.2 0.3 0.4 0.5 0.6 0.7 0.8 0.9 1.0 1.1 1.2 1.3 1.4 1.5
Gev

FIG. 2.

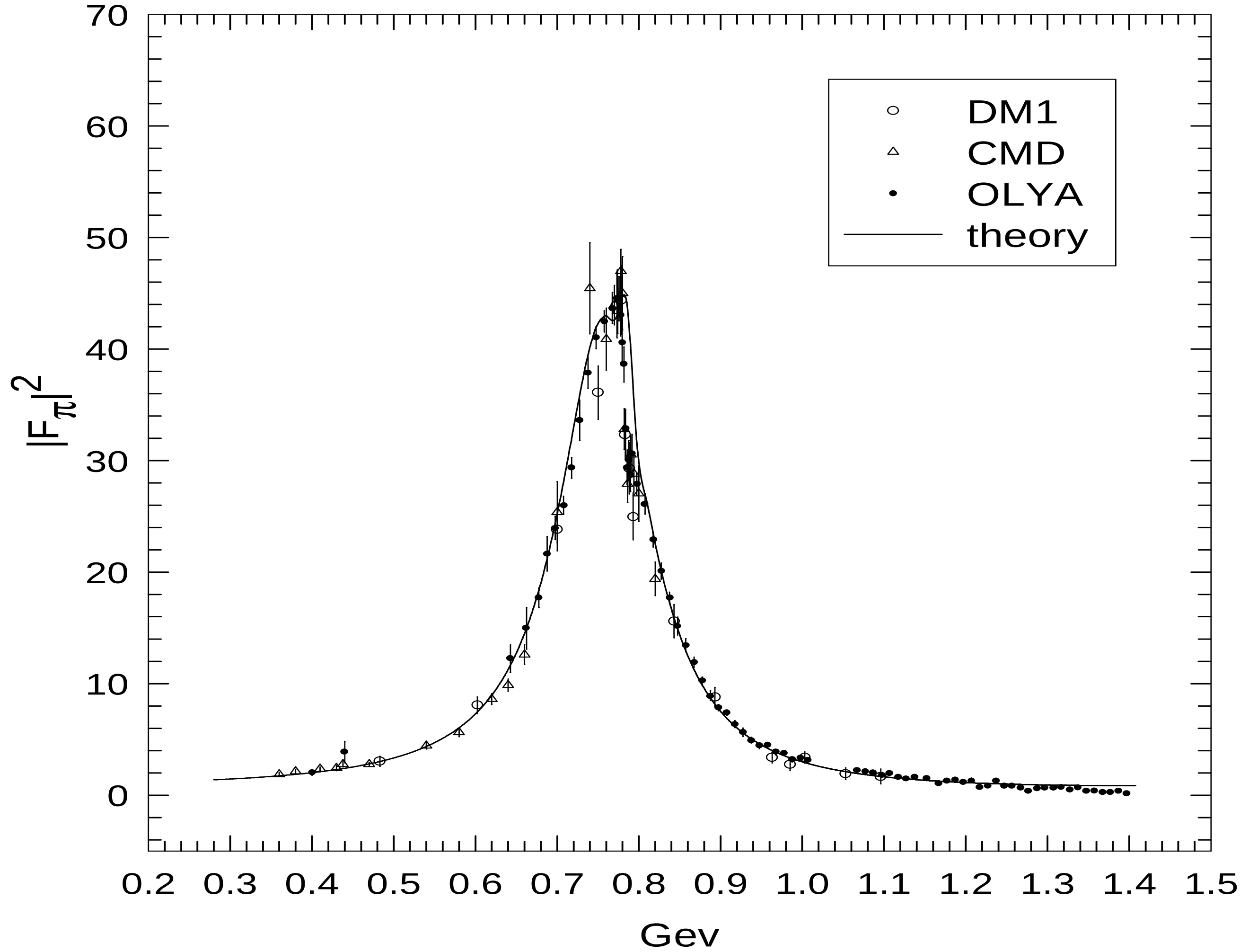
DM1
CMD
OLYA
theory
$|F_\pi|^2$
Gev
70
60
50
40
30
20
10
0
0.2 0.3 0.4 0.5 0.6 0.7 0.8 0.9 1.0 1.1 1.2 1.3 1.4 1.5

FIG. 3.

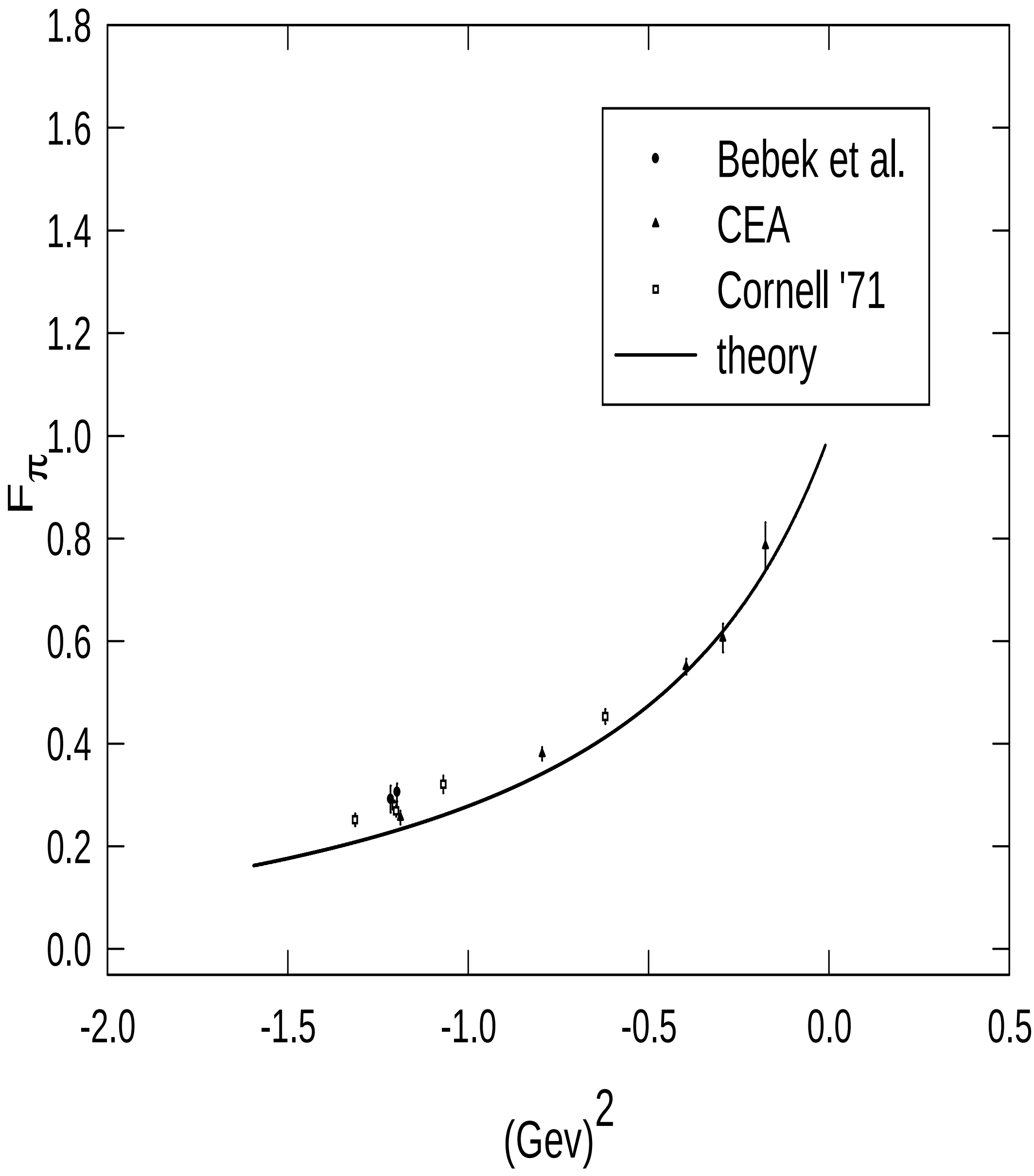
1.8
1.6
1.4
1.2
1.0
0.8
0.6
0.4
0.2
0.0
F_π
Bebek et al.
CEA
Cornell '71
theory
-2.0
-1.5
-1.0
-0.5
0.0
0.5
(Gev)^2

FIG. 4.

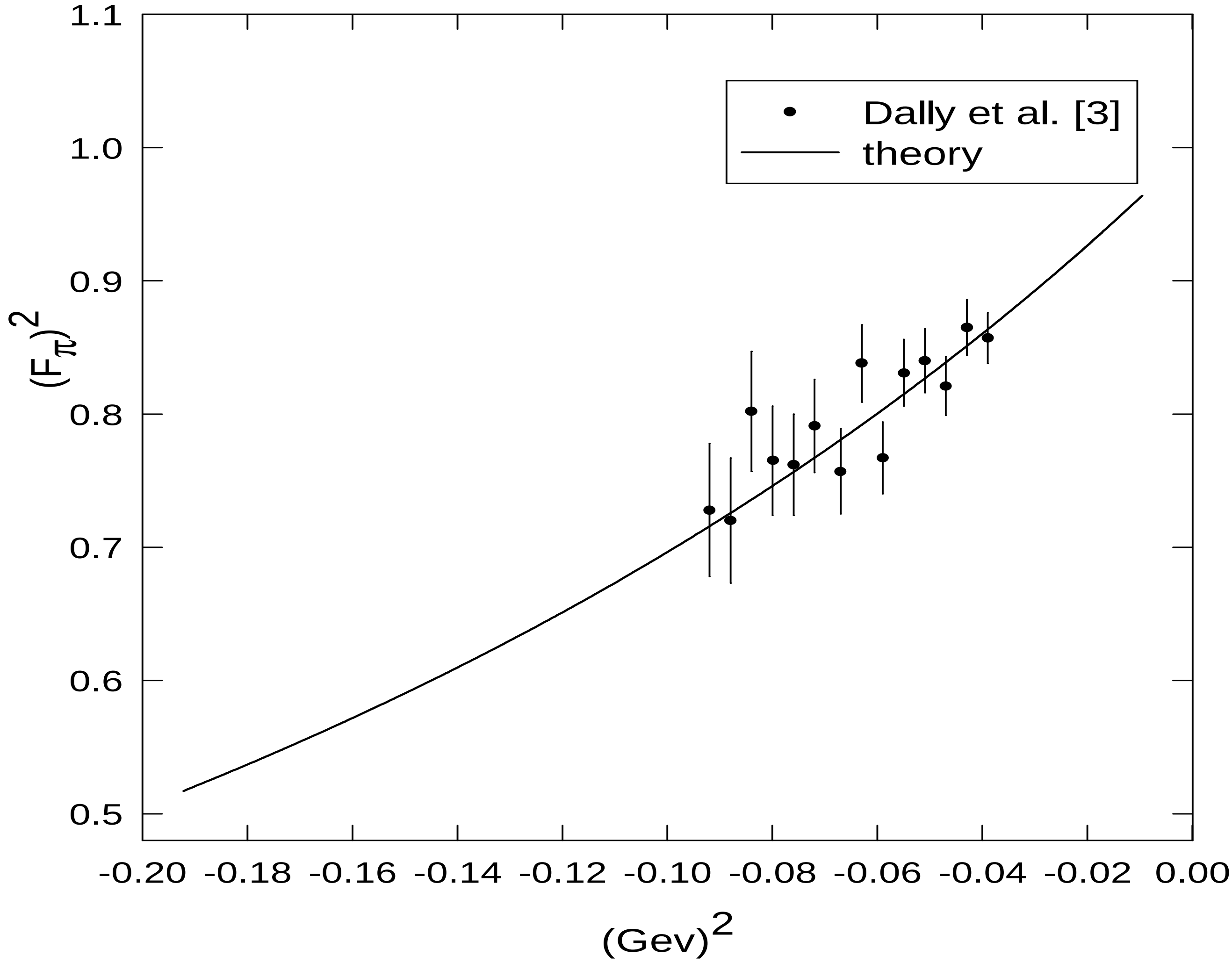

1.1
1.0
0.9
0.8
0.7
0.6
0.5
$(F_\pi)^2$
Dally et al. [3]
theory
-0.20 -0.18 -0.16 -0.14 -0.12 -0.10 -0.08 -0.06 -0.04 -0.02 0.00
$(\mathrm{Gev})^2$

FIG. 5.

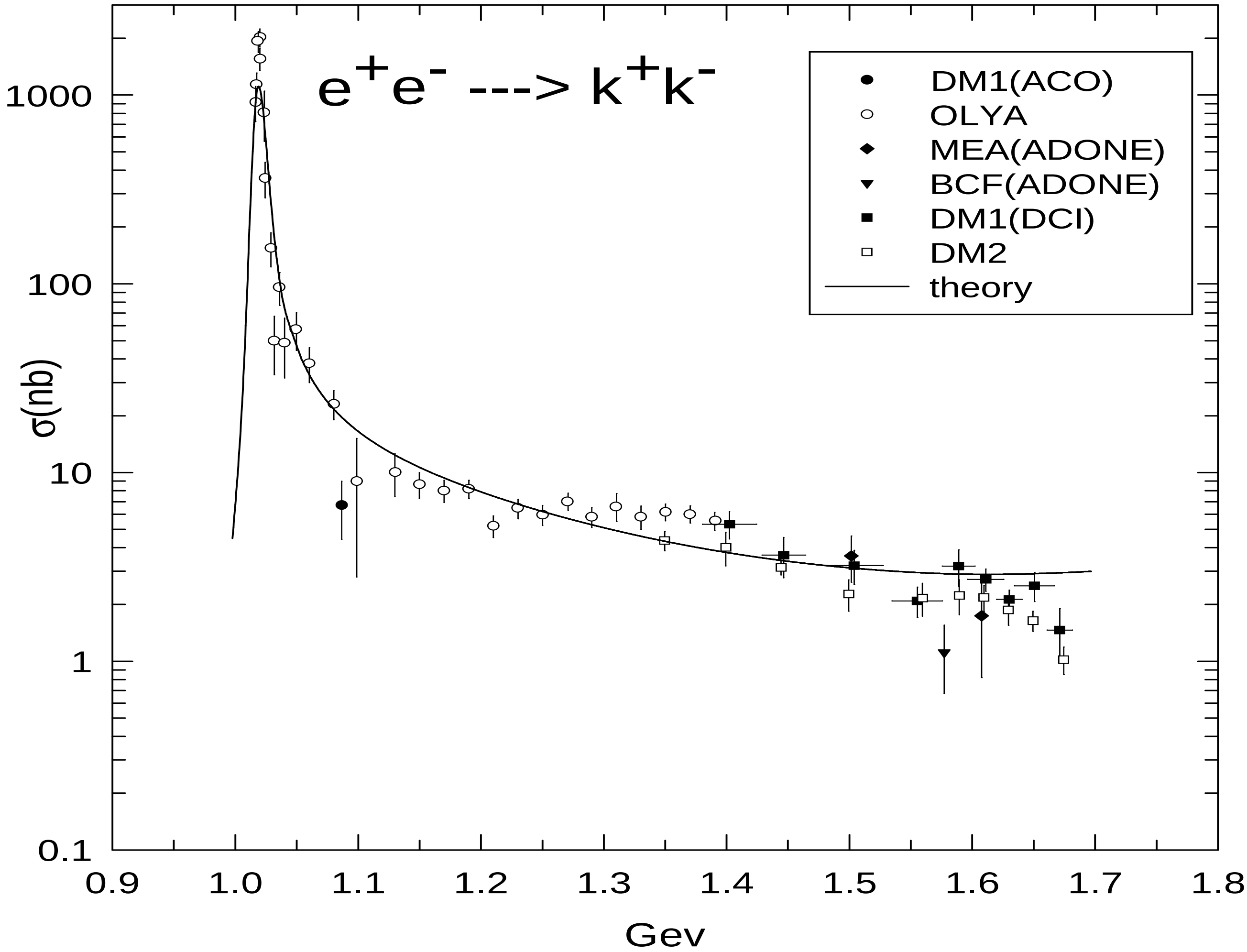

e+e- ---> k+k-
DM1(ACO)
OLYA
MEA(ADONE)
BCF(ADONE)
DM1(DCI)
DM2
theory
σ(nb)
1000
100
10
1
0.1
0.9
1.0
1.1
1.2
1.3
1.4
1.5
1.6
1.7
1.8
Gev

FIG. 6.

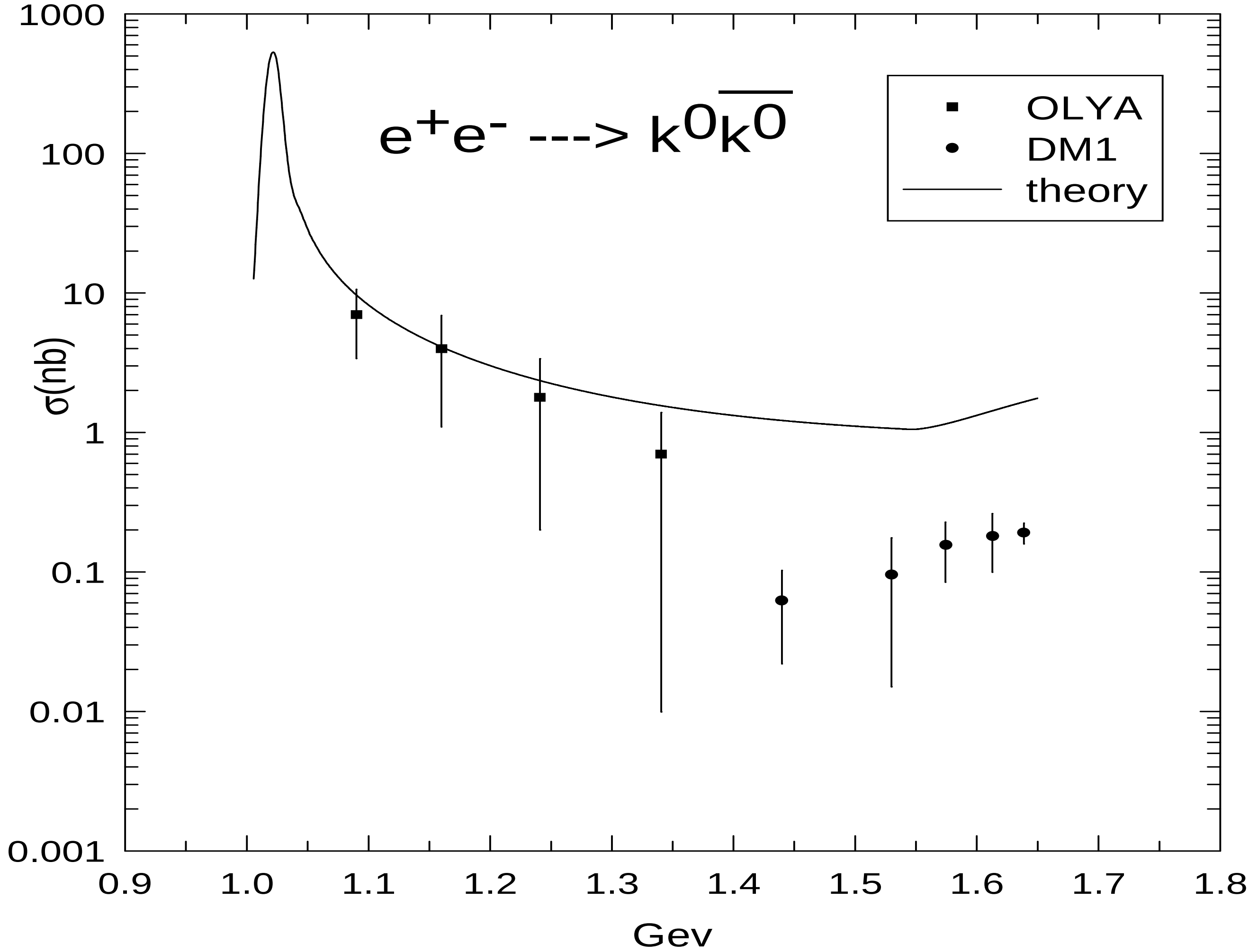

1000
100
10
1
0.1
0.01
0.001
σ(nb)
0.9
1.0
1.1
1.2
1.3
1.4
1.5
1.6
1.7
1.8
Gev
e^+e^- ---> $k^0\overline{k^0}$
OLYA
DM1
theory

FIG. 7.

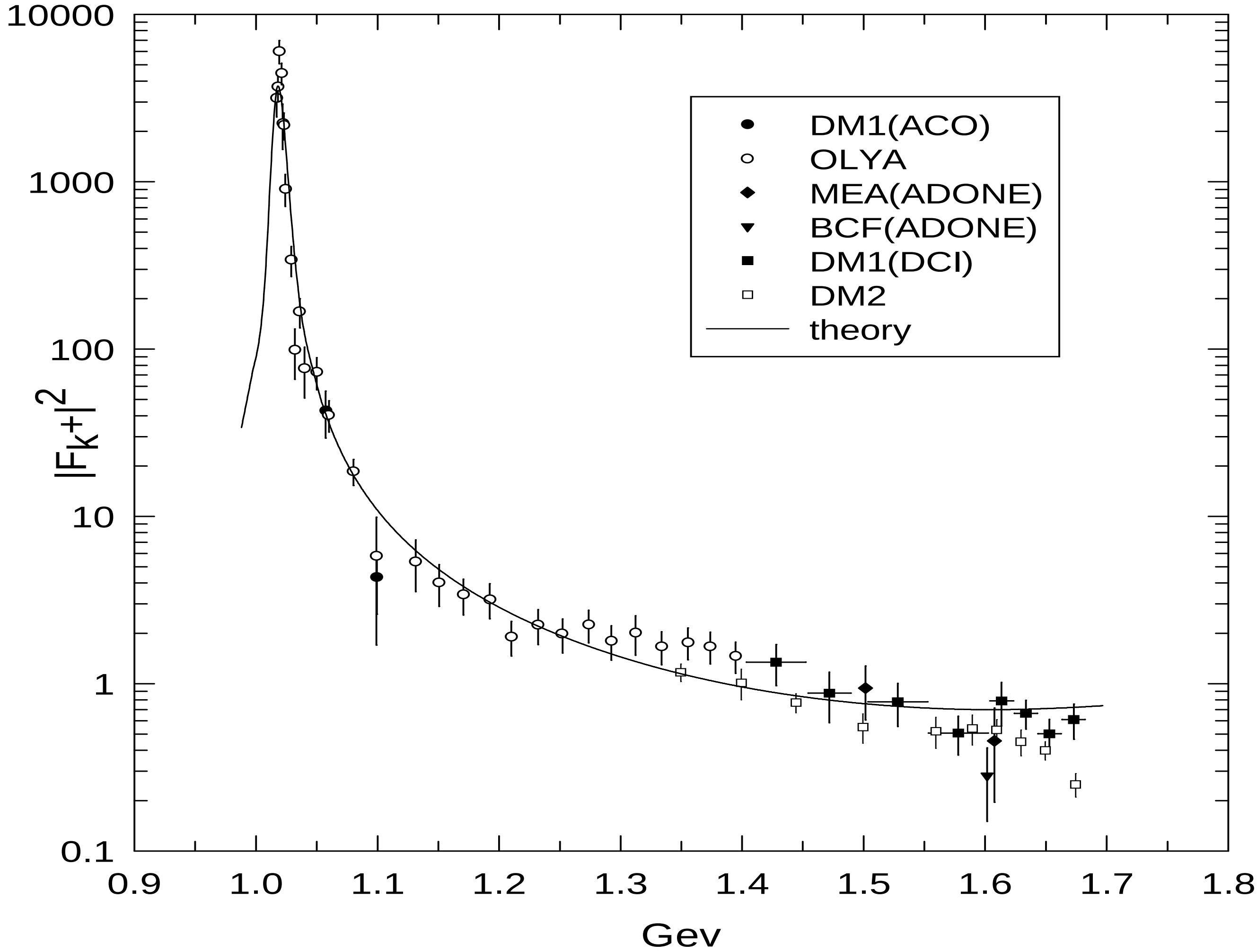

10000
1000
100
10
1
0.1
$|F_{K^+}|^2$
0.9
1.0
1.1
1.2
1.3
1.4
1.5
1.6
1.7
1.8
Gev
DM1(ACO)
OLYA
MEA(ADONE)
BCF(ADONE)
DM1(DCI)
DM2
theory

FIG. 8.

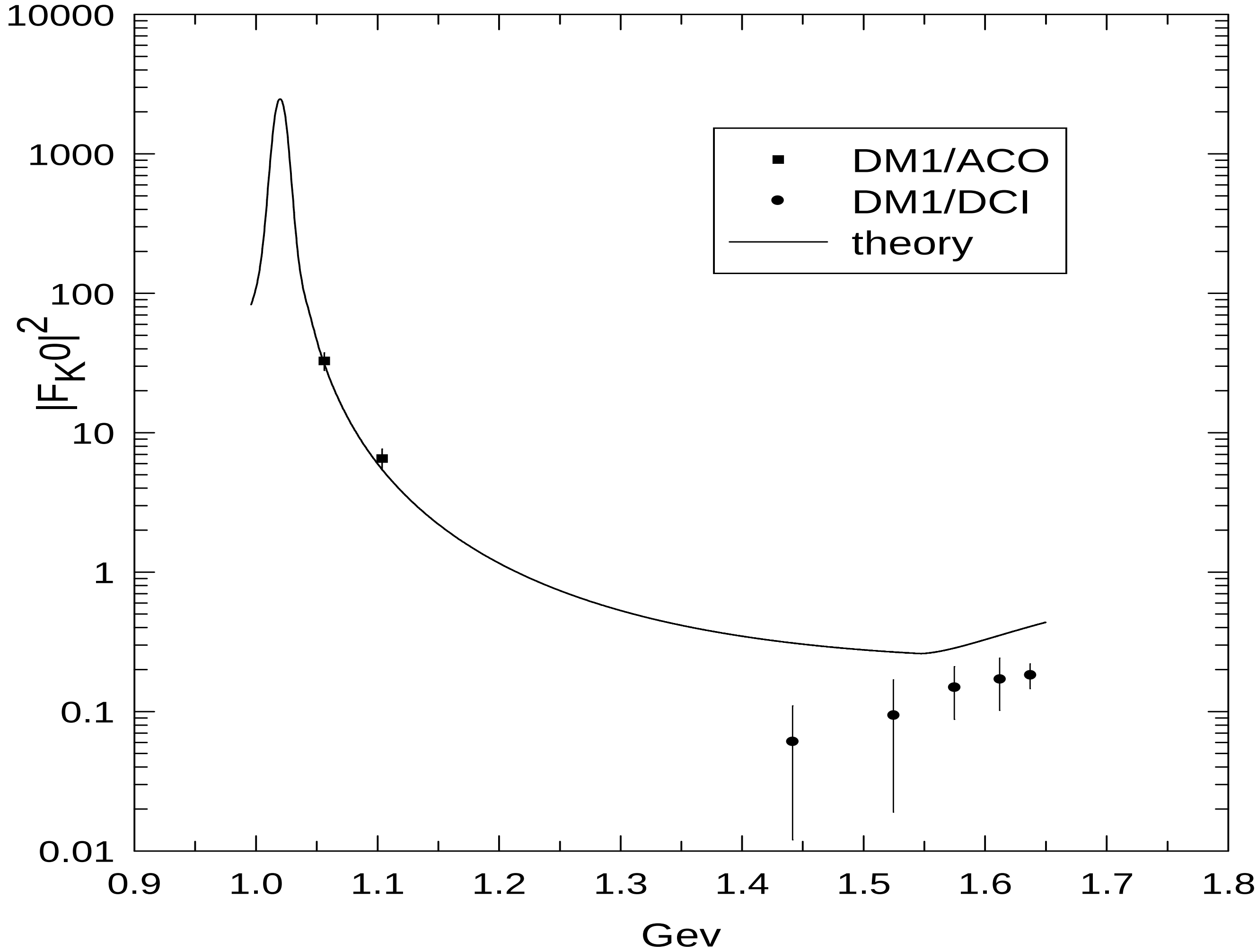

10000
1000
100
10
1
0.1
0.01
$|F_{K^0}|^2$
DM1/ACO
DM1/DCI
theory
0.9
1.0
1.1
1.2
1.3
1.4
1.5
1.6
1.7
1.8
Gev

FIG. 9.

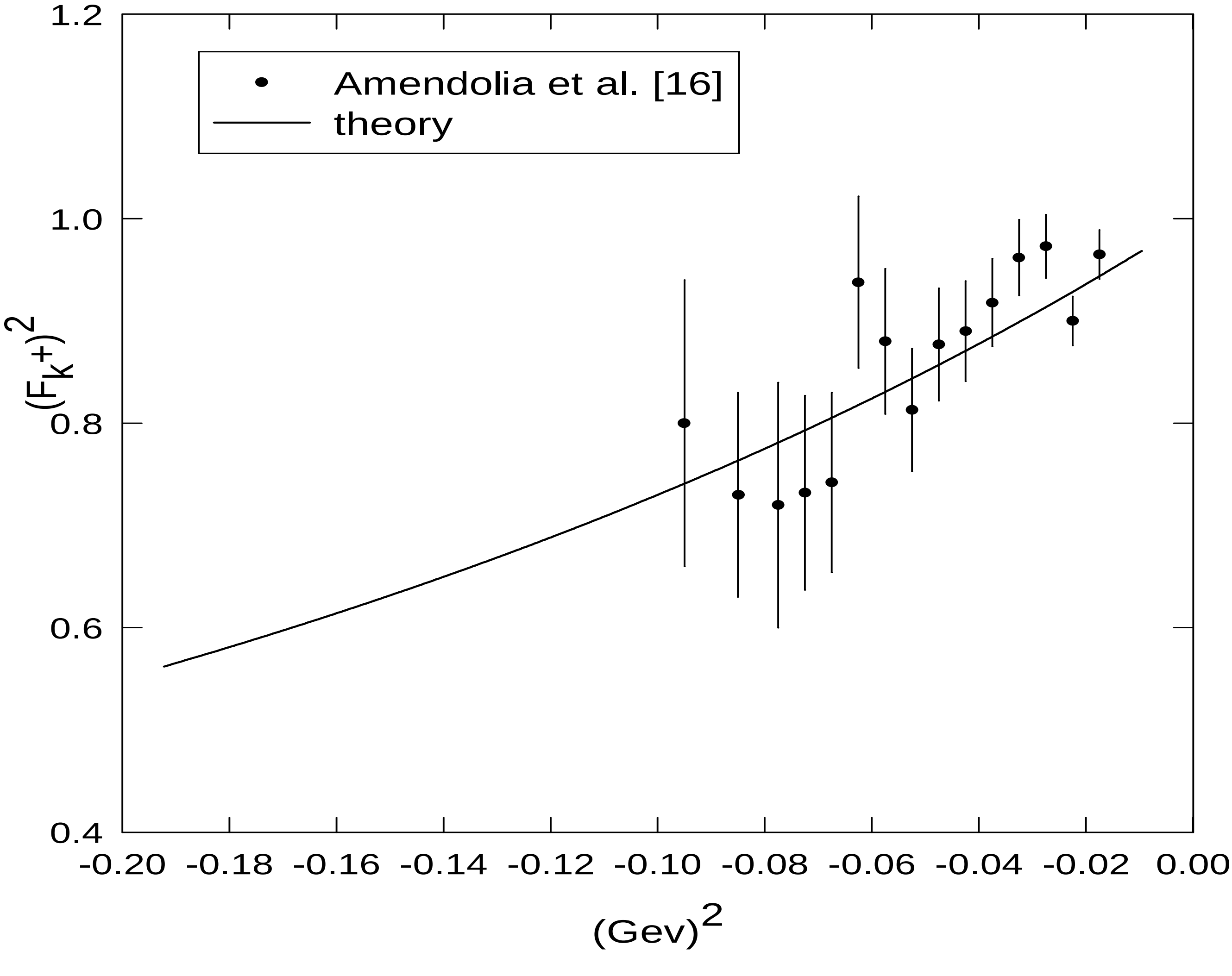

Amendolia et al. [16]
theory
1.2
1.0
0.8
0.6
0.4
$(F_{k^+})^2$
-0.20 -0.18 -0.16 -0.14 -0.12 -0.10 -0.08 -0.06 -0.04 -0.02 0.00
$(\mathrm{Gev})^2$

FIG. 10.